AMSE JOURNALS-AMSE IIETA publication-2017-Series: Modelling B; Vol. 86; N°2; pp 396-405
Submitted Mar. 03, 2017; Revised Apr. 27, 2017; Accepted May 08, 2017

Parametric Study on Deformation and Stability of Geocell-Reinforced Retaining Walls

*Fei Song, **Yuying Li, ***Jian Zhao, ****Zewei Yang

*Associate professor, Institute of Geotechnical Engineering, School of Highway Engineering, Chang'an University, Xi'an 710064, China (songf1980@163.com)
**Postgraduate, Institute of Geotechnical Engineering, School of Highway Engineering, Chang'an University, Xi'an 710064, China
***Senior Engineer, Guizhou Electric Power Design and Research Institute, Guiyang 550002, China
****Engineer, Guizhou Electric Power Design and Research Institute, Guiyang 550002, China

Abstract

This paper conducts the model tests of Chen and Chiu (2008) to validate the effect of Abaqus-based numerical model for geocell-reinforced retaining walls, and, explores how weld spacing, geocell height, and geocell tensile strength affect the horizontal displacement and the vertical settlement of geocell reinforced retaining walls (GRRWs) through the analysis of numerical simulation results. It is revealed that the horizontal displacement and the vertical settlement are correlated positively with geocell pocket size but negatively with geocell tensile strength, while the geocell height has little impact on the deformation behavior of the GRRWs.

Key words

Geocell-reinforced retaining walls (GRRWs), Horizontal displacement, Vertical settlement, Weld spacing, Height, Tensile strength.

1. Introduction

Featuring light weight, simple construction, beautification effect and ecological friendliness, geocell-reinforced retaining walls (GRRWs) have a wide prospect in the embankment protection.

Many scholars have conducted valuable research on the GRRWs, including but not limited to Bathurst and Crowe [1], Chen and Chiu [2], Chen et al. [3], Racana et al. [4], Song et al. [5-8], Xie and Yang [9], Among them, Chen and Chiu, Chen et al. performed small-scale model tests and numerical simulation to examine various parameters, such as facing inclination, type of surface, extra reinforcement and the layout of horizontal displacement and vertical settlement. Through centrifuge model tests, Song et al. investigated the failure mechanism and the effect of aspect ratio (the ratio of width to height of the wall) and slope inclination angle on the stability of the GRRWs. Song et al. studied the failure mode and the optimal sectional form of the GRRWs by the geotechnical FEM software Plaxis, and applied the proposed new retaining structure in a Chinese airport relocation project.

Nevertheless, rarely has any scholar systematically discussed how the pocket size, the height and the tensile strength of geocell influence the horizontal displacement and the vertical settlement of the GRRWs. To make up the gap, the author conducted the model tests of Chen and Chiu to validate the effect of Abaqus-based numerical model for the GRRWs, and, explored how weld spacing, geocell height, and geocell tensile strength affect the horizontal displacement and the vertical settlement of such walls.

2. Validation of the Numerical Model

2.1 Model and Parameters

This section simulates the model test results of Chen and Chiu on the GRRWs. An elastic-plastic model obeying the Drucker–Prager yield criterion was adopted for the soil. The yielding function of the criterion is provided below and the yielding surface is illustrated in Figure 1. [10]

$$F = t - p\tan\beta - d = 0 \tag{1}$$

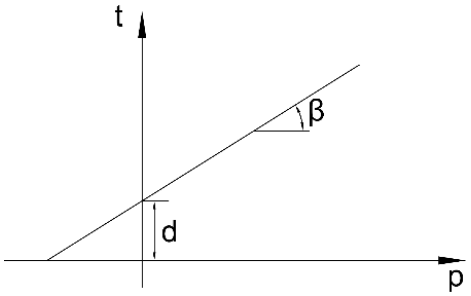

Fig.1. Yielding Surface of the Drucker-Prager Yield Criterion

The calculation parameters of the soil are listed in Table 1. Under the plane strain and plane stress condition and following the associated flow rule, the parameters of Drucker-Prager model can be obtained based on those of Mohr-Coulomb model through the following equations:

$$\tan\beta = \frac{\sqrt{3}\sin\varphi}{\sqrt{1+\frac{1}{3}\sin^2\varphi}} \tag{2}$$

$$\frac{d}{c} = \frac{\sqrt{3}\cos\varphi}{\sqrt{1+\frac{1}{3}\sin^2\varphi}} \tag{3}$$

where c and φ are the cohesion and the internal friction angle of the soil, respectively. Figure 1 explains the meanings of d and β in the Drucker-Prager model. Then, the author selected a linear elastic model to simulate the behaviour of the geocell. The geometric and mechanical parameters of the geocell used in the model tests of Chen and Chiu (2008) are shown in Table 2. All geocell pockets are in square shape. The soil was meshed into eight-node hexahedral elements (C3D8), while the geocell was modelled as four-node 3D membrane elements (M3D4) with a normal strength but no bending strength. In other words, the membrane elements can only resist tensile forces, but cannot withstand compressive or bending forces. That is why such elements are often used to simulate soil reinforcement.

Tab.1. Calculation Parameters of the Soil

	Elastic modulus E (MPa)	Unit weight γ (KN/m^3)	Poisson's ratio μ	Cohesion c (kPa)	Internal friction angle φ (º)
Sand backfill	13.88	15.3	0.33	0	44
Foundation	300	15.3	300	100	48

Tab.2. Geometric and Mechanical Parameters of Geocell

	Shape	Thickness (mm)	Height (cm)	Tensile stiffness (Mpa)	Span between the welded spots (cm)
Model 2	Square	1.3	10	60.55	13.2
Model 3	Square	1.3	10	60.55	13.2
Model 5	Square	1.3	5	15.14	6.6
Model 6	Square	1.3	5	15.14	6.6

The sketch maps of models 2, 3, 5 and 6 are presented in Figure 2. It can be seen that models 2 and 3 each has 8 geocell layers, while models 5 and 6 each has 16 geocell layers. The four models were established in Abaqus according to the geometric sizes in Figure 2.

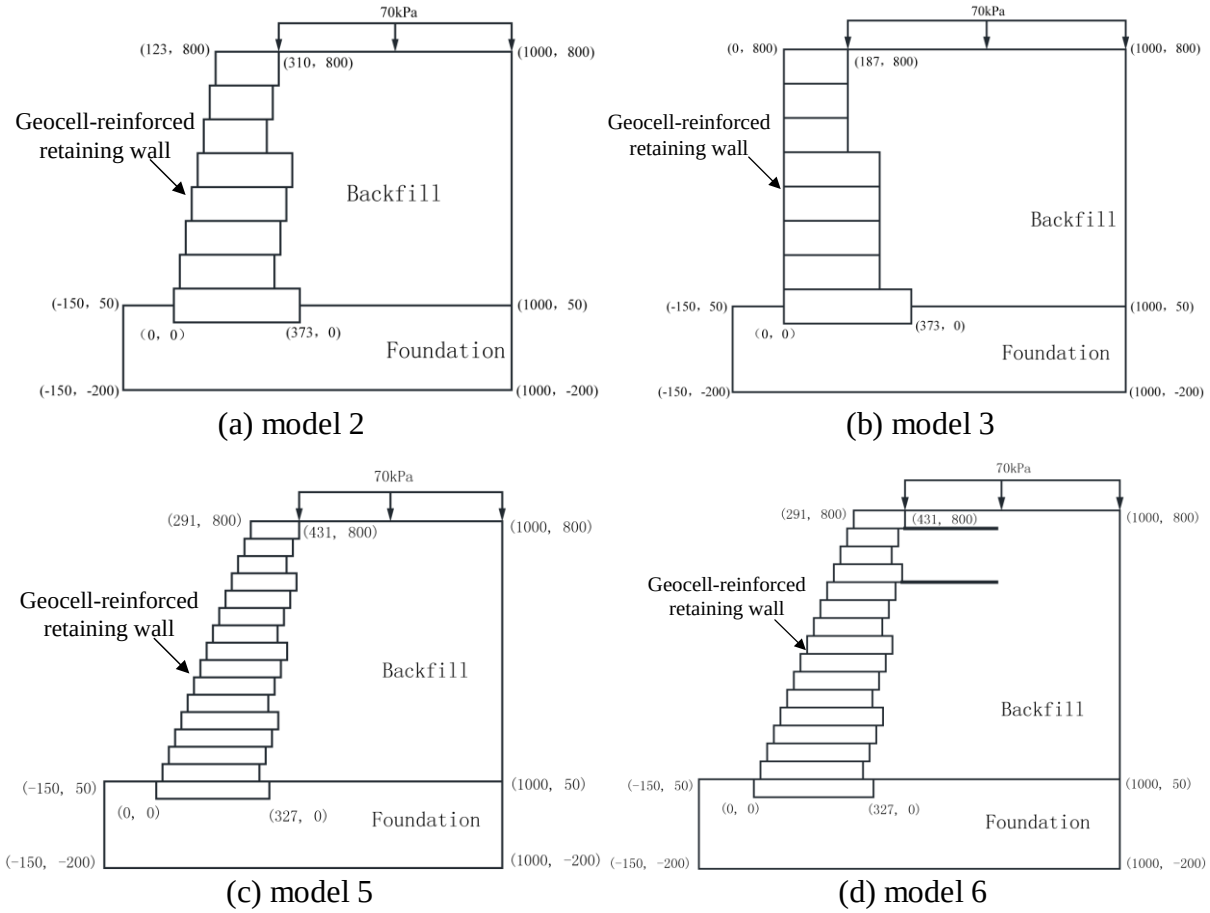

Fig.2. Sketch Maps of GRRW Models (unit: mm)

2.2 Results and Discussion

The horizontal wall facing displacements of the four models were calculated and contrasted to the results (Figure 3). As shown in Figure 3, the calculated displacements are close to the measured results, showing the validity and effectiveness of the numerical models.

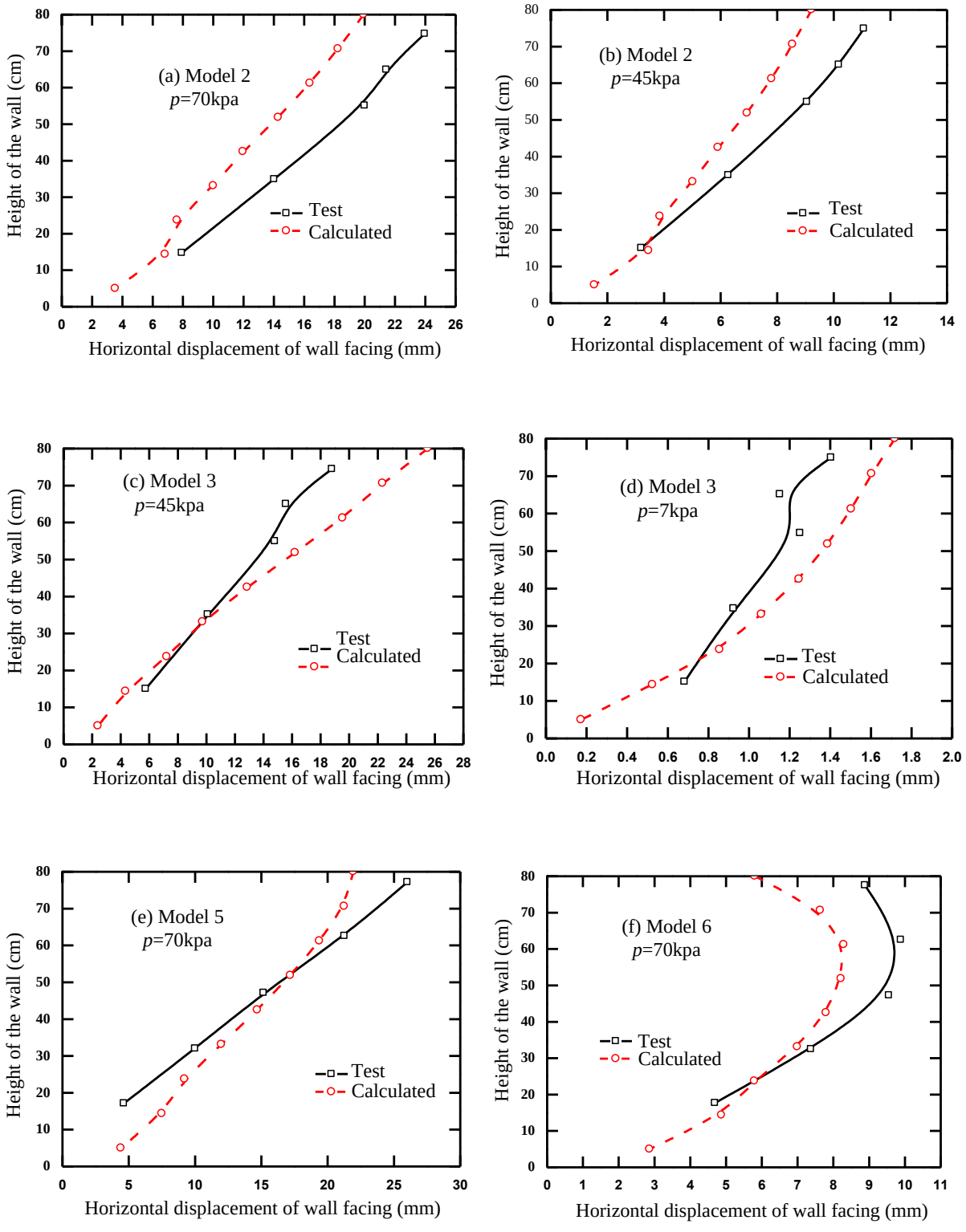

Fig.3. Comparison of Calculated and Measured Displacements

3. Parametric Study on the GRRWs

3.1 Model and Parameters

Parametric study was conducted to disclose the effect of weld spacing, geocell height, and geocell tensile strength on the horizontal displacement of the GRRWs. Figure 4 shows the wall model formulated by Abaqus. The soil was treated with an elastic-plastic model obeying the Mohr-Coulomb criterion. The parameters of the soil are given in Table 3. The behaviour of the geocell was modelled by a linear elastic model. All geocell pockets are in square shape. The parameters of the basic model include: geocell flim thickness (1.2mm), tensile modulus (500MPa), weld spacing (80cm), and geocell height (20cm).

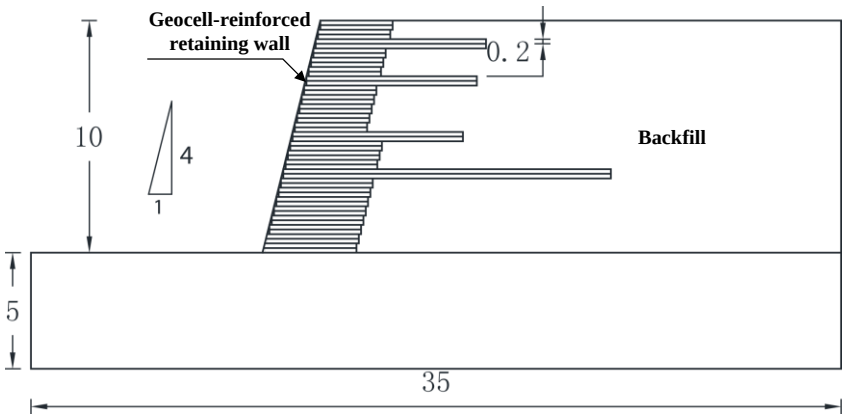

Fig.4. Sketch Map of the Simulated GRRW (unit: m)

Tab.3. Parameters of the Soil

Elastic modulus E(MPa)	Unit weight γ(KN/m^3)	Poisson's ratio μ	Cohesion c(kPa)	Internal friction angle φ(º)
15	17.6	0.35	42	10

3.2 Effect of Geocell Pocket Size

As mentioned above, the geocell pockets are all in square shape. The equivalent diameter (d) was obtained from a circle of the same size with the square. Hence, equivalent diameter was calculated as 22.57cm, 33.85cm and 45.14cm corresponding to the weld spacing of 40cm, 60cm, and 80cm. The other geometric and mechanical parameters are the same with the basic model. Figures 5 and 6 record the horizontal wall facing displacements and the vertical slope crest settlements at different geocell pocket sizes, respectively. According to the figures, both horizontal displacement and vertical settlement decrease with the geocell pocket size. The maximum

horizontal displacement is 27% smaller than that of unreinforced slope at the equivalent diameter of 22.57cm.

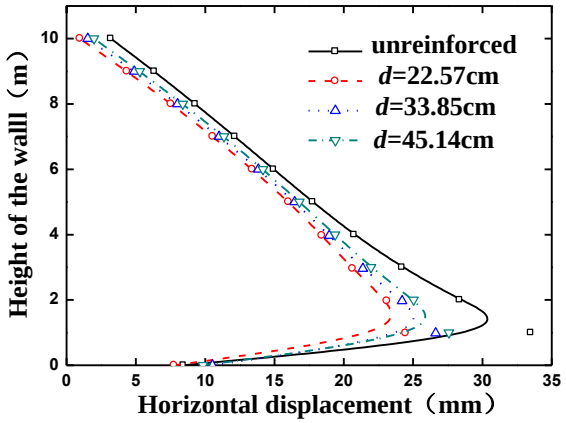

Fig.5. Effect of Geocell Pocket Size on the Horizontal Displacement

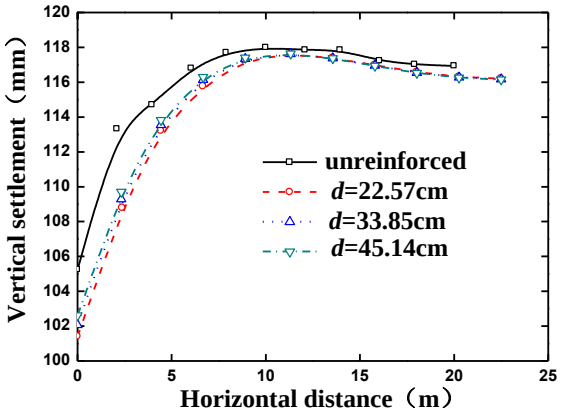

Fig.6. Effect of Geocell Pocket Size on the Vertical Settlement

3.3 Effect of Geocell Tensile Strength

The author also examined how the horizontal displacement of the reinforced slope was affected by the tensile strength of the geocell film. The tensile modulus *E* of the geocell was set to 500MPa, 800MPa, 1000MPa, 1200MPa, 1500MPa, 1800MPa, 2000MPa, 2200MPa and 2500MPa, respectively. Figures 7 and 8 illustrate the horizontal displacement and the vertical settlement of the GRRW at different geocell tensile strengths, respectively. As can be seen from these figures, the horizontal displacement and vertical settlement decrease with the increase of the tensile strength. However, the decline becomes minimal when the tensile modulus exceeds 1,800MPa. Compared to the unreinforced slope, the GRRW undergoes 35.9% of reduction in the maximum displacement at the geocell tensile modulus of 2,500MPa.

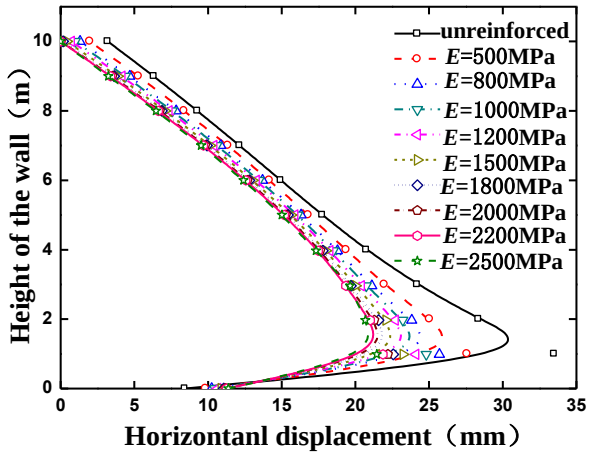

Fig.7. Horizontal Wall Facing Displacement at Different Tensile Strengths

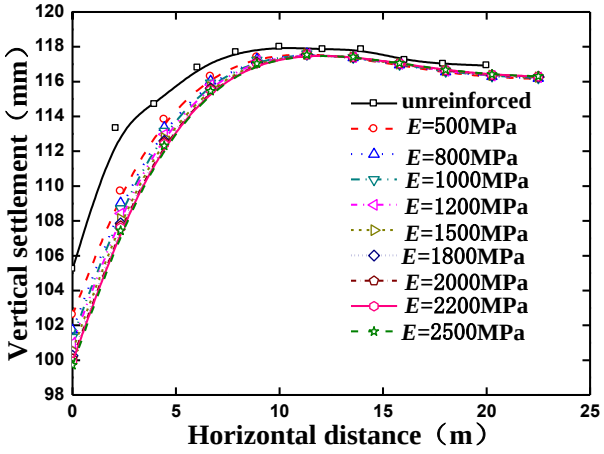

Fig.8. Vertical Slope Crest Settlement of Slope Crest at Different Tensile Strengths

3.4 Effect of Geocell Height

This section computs the horizontal displacements of the slope reinforced with geocell layers of different heights. The geocell height *h* was set to 10cm, 20cm and 40cm, respectively. The other geometric and mechanical parameters are the same with the basic model. Figures 9 and 10 show the horizontal displacement and the vertical settlement of the GRRW at different geocell heights, respectively. It can be inferred that both the horizontal displacement and the vertical settlement remain almost unchanged despite the variation in geocell height. A possible explanation lies in the tight fit between geocell layers of the GRRW. The height of the single geocell layer has little to do with the deformation behaviour of the wall as long as the wall height and the soil compactness in geocell pockets remain the same.

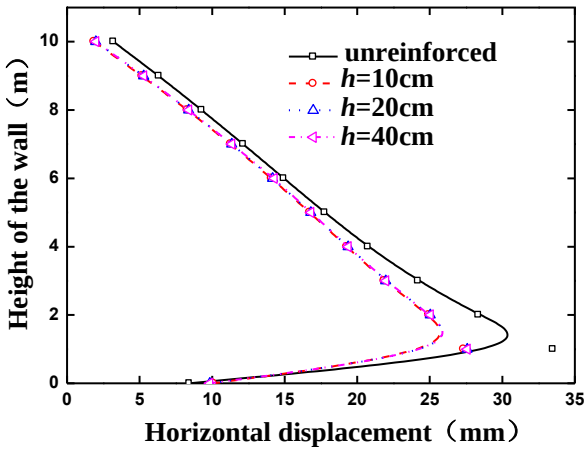

Fig.9. Horizontal Wall Facing Displacement at Different Geocell Heights

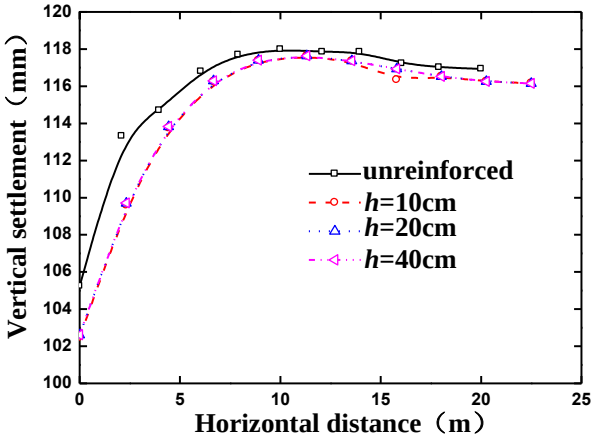

Fig.10. Vertical Slope Crest Settlement at Different Geocell Heights

Conclusion

In light of the model test results of Chen and Chiu (2008), this paper validates the effect of a finite element method for GRRW reproduction, and relies on the method to explore the effect of geocell pocket size, geocell height and geocell tensile strength on the horizontal displacement and the vertical settlement of the retaining wall. Through the analysis on the numerical simulation results, the author arrived at the following conclusions:

(1) Both horizontal displacement and vertical settlement decrease with the geocell pocket size. The maximum horizontal displacement is 27% smaller than that of unreinforced slope at the equivalent diameter of 22.57cm.

(2) The horizontal displacement and vertical settlement decrease with the increase of the tensile strength. However, the decline becomes minimal when the tensile modulus exceeds 1,800MPa.

(3) The height of the single geocell layer has little to do with the deformation behaviour of the wall as long as the wall height and the soil compactness in geocell pockets remain the same.

Acknowledgements

This research is made possible by the generous support from the Ministry of Housing and Urban-Rural Development of the People's Republic of China (No. 2015-K2-008).

References

1. R.J. Bathurst, R.E. Crowe, Recent case histories of flexible geocell retaining walls in North America, 1992, Recent case histories of permanent geosynthetic-reinforced soil retaining walls, pp. 3-19.
2. R.H. Chen, Y.M. Chiu, Model tests of geocell retaining structures, 2008, Geotextiles and Geomembranes, no. 26, pp. 56-70.
3. R.H. Chen, C.P. Wu, F.C. Huang, C.W. Shen, Numerical analysis of geocell-reinforced retaining structures, 2013, Geotextiles and Geomembranes, no. 39, pp. 51-62.
4. N. Racana, R. Gourve` s, M. Gre´diac, Mechanical behavior of soil reinforced by geocells, 2001, In: Proceedings of the International Symposium on Earth Reinforcement, Japan, pp. 437-442.
5. F. Song, G.R. Cao, L.Y. Zhang, X. M. Tan, Numerical analysis of failure mode of geocell flexible retaining Wall, 2013, ASCE Geotechnical Special Publication, no. 232, pp. 136-145.
6. F. Song, Y.L. Xie, Y.F. Yang, X.H. Yang, Analysis of failure of flexible geocell-reinforced retaining walls in the centrifuge, 2014a, Geosynthetics International, vol. 21, no. 6, pp. 342-351.
7. F. Song, Y.L. Li, K. Zhang, L.Y. Zhang, Study on the optimum sectional form of geocell reinforced retaining wall, 2014b, International Journal of Earth Sciences and Engineering, vol. 7, no, 2, pp. 571-577.
8. F. Song, H.B. Hu, L.Q. Ma, Y.B. Zhao, Engineering application of a new type geocell retaining wall with variable cross-section, 2016, International Journal of Earth Sciences and Engineering, vol. 9, no. 4, pp. 1602-1606.
9. Y.L. Xie, X.H. Yang, Characteristics of a new-type geocell flexible retaining wall, 2009, Journal of Materials in Civil Engineering, ASCE, vol. 21, no. 4, pp. 171-175.
10. M. Okuyama, T. Ajiki, K. Yazawa, K. Kaneko, M. Horie, K. Kumagai, Field observation of geocell reinforced retaining walls after the Niigataken Chuetsu-oki earthquake, 2007, Geosynthetics Engineering Journal, no. 22, 239-242.